8-1-2020

Glutamate and Dysconnection in the Salience Network: Neurochemical, Effective Connectivity, and Computational Evidence in Schizophrenia

Roberto Limongi
The University of Western Ontario

Peter Jeon
The University of Western Ontario

Michael Mackinley
The University of Western Ontario

Tushar Das
Fanshawe College

Kara Dempster
Dalhousie University, Faculty of Medicine

See next page for additional authors

Archival Report

Biological Psychiatry

Glutamate and Dysconnection in the Salience Network: Neurochemical, Effective Connectivity, and Computational Evidence in Schizophrenia

Roberto Limongi, Peter Jeon, Michael Mackinley, Tushar Das, Kara Dempster, Jean Théberge, Robert Bartha, Dickson Wong, and Lena Palaniyappan

ABSTRACT

BACKGROUND: Functional dysconnection in schizophrenia is underwritten by a pathophysiology of the glutamate neurotransmission that affects the excitation-inhibition balance in key nodes of the salience network. Physiologically, this manifests as aberrant effective connectivity in intrinsic connections involving inhibitory interneurons. In computational terms, this produces a pathology of evidence accumulation and ensuing inference in the brain. Finally, the pathophysiology and aberrant inference would partially account for the psychopathology of schizophrenia as measured in terms of symptoms and signs. We refer to this formulation as the 3-level hypothesis.

METHODS: We tested the hypothesis in core nodes of the salience network (the dorsal anterior cingulate cortex [dACC] and the anterior insula) of 20 patients with first-episode psychosis and 20 healthy control subjects. We established 3-way correlations between the magnetic resonance spectroscopy measures of glutamate, effective connectivity of resting-state functional magnetic resonance imaging, and correlations between measures of this connectivity and estimates of precision (inherent in evidence accumulation in the Stroop task) and psychopathology.

RESULTS: Glutamate concentration in the dACC was associated with higher and lower inhibitory connectivity in the dACC and in the anterior insula, respectively. Crucially, glutamate concentration correlated negatively with the inhibitory influence on the excitatory neuronal population in the dACC of subjects with first-episode psychosis. Furthermore, aberrant computational parameters of the Stroop task performance were associated with aberrant inhibitory connections. Finally, the strength of connections from the dACC to the anterior insula correlated negatively with severity of social withdrawal.

CONCLUSIONS: These findings support a link between glutamate-mediated cortical disinhibition, effective-connectivity deficits, and computational performance in psychosis.

Keywords: Dynamic causal models, Dysconnection hypothesis, Effective connectivity, Glutamate hypothesis, Predictive coding, Schizophrenia

https://doi.org/10.1016/j.biopsych.2020.01.021

The glutamate hypothesis (1–4) has been a central focus of interest in the study of the psychopathology of schizophrenia for more than 20 years. It states that dysfunction of glutamatergic neurotransmission is associated with signature symptoms of schizophrenia. This dysfunction is likely caused by NMDA receptor hypofunction (i.e., glutamate hypofunction) in inhibitory gamma-aminobutyric acidergic (GABAergic) interneurons, which would lead to an increase in the synaptic gain of excitatory neurons [the disinhibition hypothesis (5,6)]. Abnormal increase of synaptic gain is also conceptualized as a disruption of the excitation-inhibition balance, which, as described below, rests at the core of the dysconnection hypothesis (7) within the theoretical framework of "the Bayesian brain"[1] (8).

The dysconnection hypothesis suggests that the psychopathology of schizophrenia should be studied at 3 levels of analysis: neurochemical, effective-connectivity

[1]This Bayesian account tends to suggest the existence of an inner controller (e.g., a central executive), which inevitably would call upon the homunculus fallacy. However, the dysconnection hypothesis is nested within the active inference theory under the free energy formulation. From this perspective, the homunculus fallacy dissolves in terms of autopoietic self-organization.

ISSN: 0006-3223

(network-connectivity), and computational levels. At the neurochemical level, NMDA receptor hypofunction would increase the synaptic gain in deep and superficial pyramidal cells, reflecting a decrease in the strength of intrinsic inhibitory connections (7,9). At the effective-connectivity level, a predictive coding algorithm (10), namely, hierarchical message passing between lower and higher cortical levels, would be altered in terms of aberrant backward and forward interregional connectivity strength (11). At the computational level, a suboptimal Bayesian brain (12) would overly afford confidence or precision (i.e., inverse variance) to its predictions about the external stimuli and would overestimate the reliability of the prediction errors (PEs), leading to false inferences and failures in cognitive control (13–15).

To test this hypothesis, in this work we study the relationship between cognitive-control dysfunction in schizophrenia, the effective connectivity between core nodes of the salience network (the right dorsal anterior cingulate cortex [dACC] and the right anterior insula [AI]), and the concentration of ^{1}H-magnetic resonance spectroscopy (MRS) glutamate in the dorsal anterior cingulate cortex ($[Glu]_{dACC}$). At the computational level, we compare the performance of subjects with first-episode psychosis (FEP) and healthy control (HC) subjects in the Stroop task (16), which reliably engages the dACC–AI network (17,18). Suboptimal Stroop computations in FEP are reflected in long reaction time and low response accuracy (19,20). We show that a drift-diffusion model, as a specific case of a Bayesian decision making (21), explains these suboptimal computations. At the effective-connectivity level, we show that the computational parameter associated with aberrant predictions in FEP maps onto extrinsic connections. Ultimately, we demonstrate at the neurochemical level that $[Glu]_{dACC}$ drives the dysconnection within the dACC–AI network, which, as we detail below, is an appropriate anatomical and functional motif [cf. (22)] to evaluate our 3-level hypothesis.

The dACC functionally specializes in conflict monitoring during the Stroop task (23) and is anatomically connected to the AI (24–26). Crucially, psychosis is associated with consistent structural deficits (27) as well as resting-state functional dysconnectivity in this network (28,29). Given that the AI is particularly sensitive to descending afferents from the dACC (30), we expected variations of excitation-inhibition balance resulting from the glutamatergic abnormalities within the dACC to induce dysconnectivity in the network, affecting both the intrinsic inhibitory connections of the dACC and the extrinsic connections with the AI.

Negative symptoms are regarded as the core drivers of functional deficits in schizophrenia. Nevertheless, the evidence relating glutamate to negative symptoms has been conflicting to date (31). From previous experimental work linking reduced precision of priors (relative to precision of PE) and negative symptoms (32–34), we expected negative association between effective connectivity within the two-node network and higher negative symptoms.

In summary, we used a multilateral approach to test a specific dysconnection hypothesis that has 3 related aspects. First, functional dysconnection in schizophrenia is underwritten by a pathophysiology of the glutamate neurotransmission that affects the excitation-inhibition balance in key nodes of the salience network. Physiologically, this is manifest as aberrant effective connectivity in intrinsic connections involving inhibitory interneurons. Second, in computational terms, this produces a pathology of evidence accumulation and ensuing inference in the brain—as manifest in terms of psychophysics. Third, the pathophysiology and aberrant inference partially account for the psychopathology of schizophrenia as measured in terms of symptoms and signs. We will refer to this formulation as the 3-level hypothesis and establish its validity by looking for 3-way correlations between the MRS measures of glutamate, dynamic causal modeling (DCM) measures of directed connectivity, and correlations between measures of this connectivity and estimates of precision (inherent in evidence accumulation) on the one hand and psychopathology on the other.

METHODS AND MATERIALS

Subjects

Twenty subjects with FEP and 20 HC subjects participated in the study (Tables S1 and S2). Glutamate MRS assessment could not be performed in 1 subject with FEP. Data from this subject were not analyzed. Subjects were recruited from the Prevention and Early Intervention Program for Psychosis in London, Ontario, Canada. Criteria for inclusion in the FEP group included 1) first clinical presentation with psychotic symptoms and DSM-5 (35) criteria A for schizophrenia satisfied and 2) less than 2 weeks of lifetime antipsychotic exposure. All patients with FEP received a consensus diagnosis from 3 psychiatrists (LP, KD, and the primary treatment provider) after approximately 6 months on the basis of the best estimate procedure, as described by Leckman *et al.* (36), and the Structured Clinical Interview for DSM-5. All patients satisfied criteria for schizophrenia spectrum disorder, with 15 patients satisfying DSM-5 criteria for schizophrenia and 3 for schizoaffective disorder. One subject lacked follow-up clinical data at 6 months, with the available baseline data suggesting a diagnosis of schizophreniform disorder. We use the term "first-episode psychosis" to describe the patient group to capture all the schizophrenia spectrum disorders as described above. HC participants did not report a personal history of mental illness or family history of psychotic disorders. Informed consent from participants was obtained according to the approval by Western University's Human Ethics Committee. Symptoms assessment was performed using Positive and Negative Syndrome Scale-8 items version (37) (Table S3). As detailed below, participants underwent, in this order, resting-state ^{1}H-MRS, a color version of the Stroop task, and resting-state functional magnetic resonance imaging (fMRI) inside a MAGNETOM Plus 7T MRI scanner (Siemens Corp., Erlangen, Germany) using an 8-channel transmit/32-channel receive, head-only, radiofrequency coil.

^{1}H-MRS

We measured a 4-minute block of resting-state ^{1}H-MRS in a voxel (2.0 × 2.0 × 2.0 cm) that was placed on the dACC

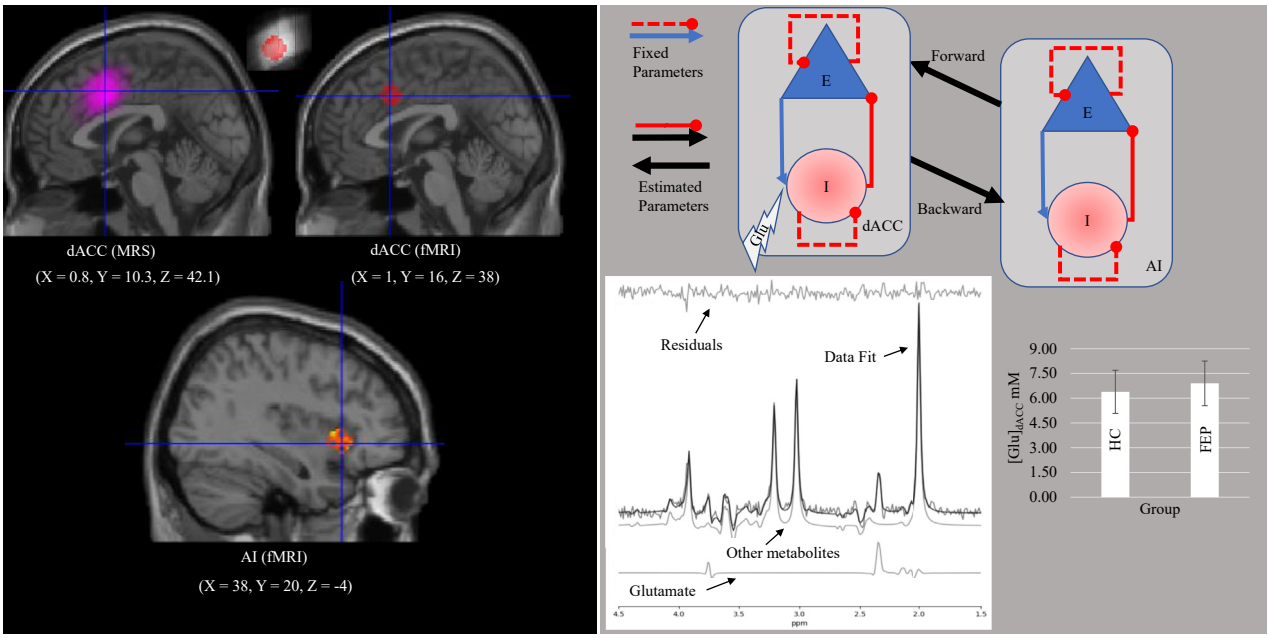

Figure 1. Voxel positioning for ^{1}H-magnetic resonance spectroscopy (MRS) measurements, sphere positioning for functional magnetic resonance imaging (fMRI) time series extraction, and 2-neuronal-population dynamic causal modeling. In the dorsal anterior cingulate cortex (dACC), the fMRI sphere falls within the MRS voxel (black box). The gray box shows the 2-neuronal-population dynamic causal modeling of the dACC–anterior insula (AI) network. Each region comprises one population of excitatory neurons (E) and one population of inhibitory neurons (I). Parameters of effective connectivity represent the influence of inhibitory to excitatory connections (assumed to be gamma-aminobutyric acidergic neurons), the influence of excitatory to inhibitory connections, the influence of self-inhibitory connections within each population, and the influence of excitatory population of one region on the excitatory population of the other region (assumed to be glutamatergic connections). Whereas excitatory-to-inhibitory connections and excitatory-to-inhibitory connections within each population parameters are fixed in the model, inhibitory-to-excitatory connections and excitatory population of one region on the excitatory population of the other region are free parameters. The small white box shows a sample spectrum obtained using ^{1}H-MRS semi-LASER (localization by adiabatic selective refocusing) with an echo time of 100 ms. A frequentist 2-sample *t* test did not reveal a statistically significant difference between the mean glutamate in the dorsal anterior cingulate cortex ($[Glu]_{dACC}$) in the first-episode psychosis (FEP) group (mean = 6.90 mM, SD = 1.35) relative to the healthy control (HC) group (mean = 6.38 mM, SD = 1.3); $t_{36.72} = 1.21$, $p = .88$. Error bars represent the standard deviations.

(Figure 1 and Figure S1) where activation was expected based on our previous work using the Stroop task (20). To locate the voxel, we used a 2-dimensional anatomical imaging sequence in the sagittal direction (37 slices, repetition time = 8000 ms, echo time = 70 ms, flip angle [α] = 120°, thickness = 3.5 mm, field of view = 240 × 191 mm; voxel control is described in the Supplemental Methods). A 32-channel combined water-suppressed spectral average was acquired using the semi-LASER (localization by adiabatic selective refocusing) ^{1}H-MRS pulse sequence (repetition time = 7500 ms) with a long echo time (100 ms)—this long echo time improves glutamate measurement in the human brain (38). Water suppression was achieved using the VAPOR (variable pulse power and optimized relaxation delays) preparation sequence, and a water-unsuppressed spectrum was also acquired for spectral postprocessing (Supplemental Methods).

Resting-State fMRI

We acquired 360 resting-state whole-brain functional images. A gradient echo-planar imaging sequence was used with phase-encoding direction = A > > P, repetition time = 1000 ms, echo time = 20 ms, flip angle = 30°, field of view = 208 mm, field of view phase = 100%, voxel dimension = 2 mm isotropic, slice thickness = 2 mm, multiband acceleration factor = 3, acquisition time = 6 minutes, 26 seconds, and number of slices = 63 (interleaved slice order).

Computational Model of the Stroop Performance

Based on our previous work (20), we were interested in the incongruent condition of the Stroop task (Supplemental Methods) in which we expected lower accuracy and longer reaction time in subjects with FEP than in HC subjects. We fit a hierarchical drift-diffusion model to the reaction time and accuracy data (Supplemental Methods). In this model, participants accumulate information and trigger a response after reaching an accumulation threshold. The model comprises 4 basic parameters representing the accumulation threshold, the starting point of the accumulation process, the accumulation (or drift) rate, and the nondecision processes.

Predictive coding maps elegantly onto the drift-diffusion model (13,21,39). Evidence accumulation corresponds to the accumulation of presynaptic afferent activity from neuronal populations encoding PEs (i.e., superficial pyramidal cells), the drift rate represents precision of ascending PE, and the starting point represents prior beliefs. Formally, corrected prior beliefs (i.e., a change in the starting point parameter) correlates with a larger drift rate, indicating more precise PE. We expected larger drift rate (i.e., aberrant precision of PE) and larger

Table 1. Summary Statistics of Accuracy and RT in the Stroop Task

		Accuracy (Proportion)		RT (s)	
Group	Condition	Mean	SD	Mean	SD
FEP	Color-only	0.99	0.07	1.06	0.27
	Congruent	0.98	0.14	0.98	0.27
	Incongruent	0.92	0.27	1.19	0.31
	Word-only	0.97	0.17	0.95	0.26
HC	Color-only	0.99	0.05	0.89	0.20
	Congruent	0.99	0.05	0.82	0.21
	Incongruent	0.98	0.14	1.04	0.25
	Word-only	1.00	0.00	0.79	0.18

FEP, first-episode psychosis; HC, healthy control; RT, reaction time.

starting point (aberrant prior beliefs) in the FEP group than in the HC group. Although we did not have a priori expectations about differences in the decision threshold and in nondecision processes, we report the differences in these parameters for completeness and post hoc interpretation. We report between-groups difference in the posterior probability (PP) of parameter estimates.

Effective Connectivity: DCM

We estimated the resting-state effective connectivity within the dACC–AI network by fitting a 2-state spectral dynamic causal model (40) to the fMRI data (41) (Supplemental Methods). We identified regions with blood oxygen–level fluctuations within frequencies ranging from 0.0078 to 0.1 Hz (42) via an F-contrast. We extracted the time series that summarized the activity within spheres (8-mm radius) in the dACC and in the AI (Figure 1 and Figure S1). Montreal Neurological Institute coordinates of these spheres were defined based on our previous works (20,43). Two-state DCM assumes excitatory and inhibitory populations of neurons within a region. Each population comprises self-inhibition connections (which are fixed parameters). Crucially, 2 free parameters are fit to the fMRI data: interregional excitatory-to-excitatory connections and within-region inhibitory-to-excitatory connections (Figure 1). Since we aimed at demonstrating the relationship between the effect of $[Glu]_{dACC}$ on inhibitory-to-excitatory connections and the ensuing consequences in the entire network, this 2-state model was sufficient to test our hypothesis despite not capturing all the circuitry constraints of cortical columns.

For each participant, a fully connected model with no exogenous inputs (c.f., task fMRI) was specified and inverted using spectral DCM. At a group level, we estimated parameters of 6 parametric empirical Bayes models (44,45) aiming to test our 3-level hypothesis against 5 alternative hypotheses. The 3-level model comprised 1) group, 2) $[Glu]_{dACC}$, 3) precision of

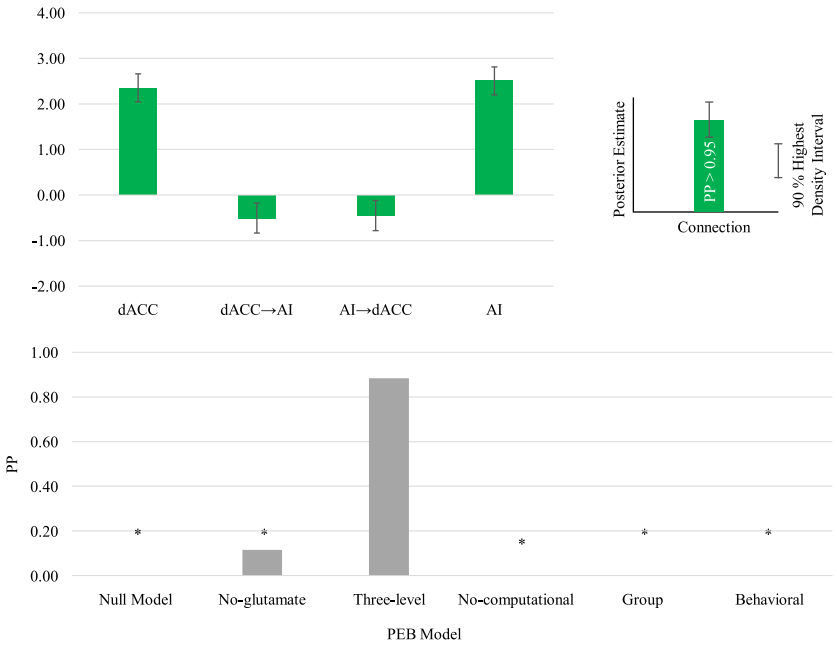

Figure 2. Bayesian model comparison results and mean parameter estimates in the dorsal anterior cingulate cortex (dACC)–anterior insula (AI) network across groups. *Posterior probability (PP) ≈ 0. PEB, parametric empirical Bayes.

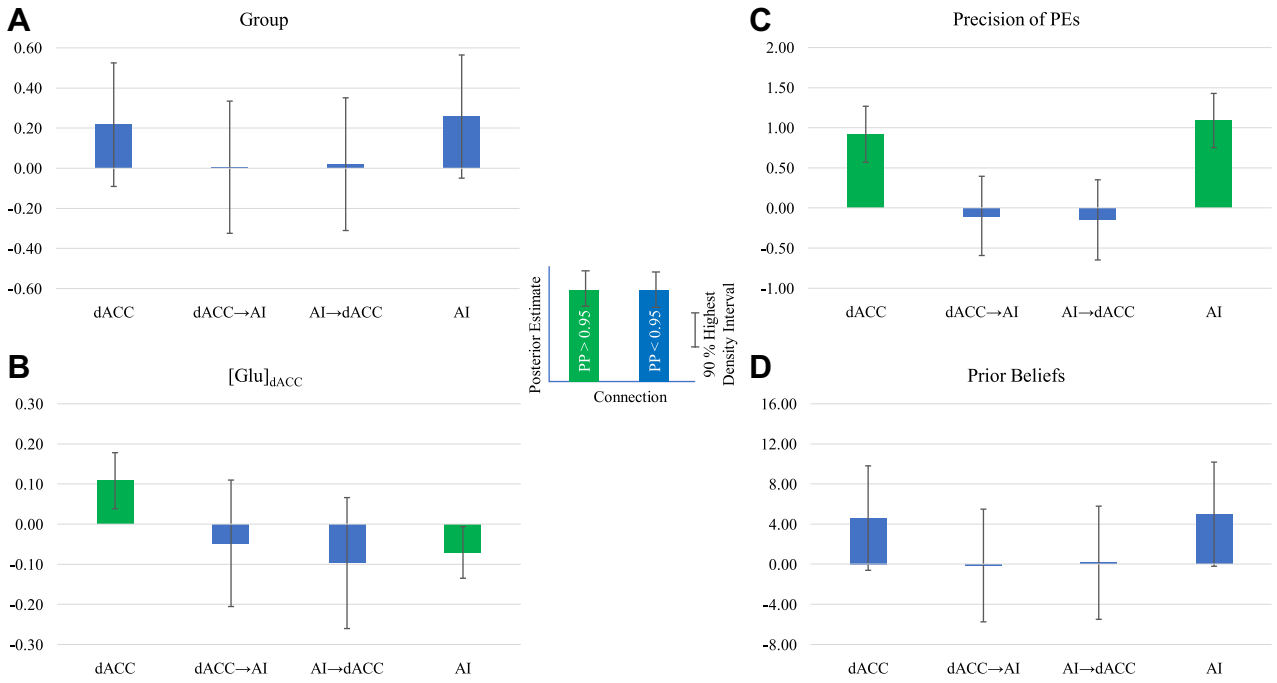

Figure 3. Main effects of the winning 3-level parametric empirical Bayes model. In **(A)**, bars represent differences between groups as defined by the effect coding (first-episode psychosis = 1, healthy control = −1). In **(B)**, **(C)**, and **(D)**, glutamate in the dorsal anterior cingulate cortex ($[Glu]_{dACC}$), precision of prediction errors (PEs), and prior beliefs (respectively) were mean centered. AI, anterior insula; PP, posterior probability.

PE, 4) prior beliefs, 5) $[Glu]_{dACC}$ × group, 6) $[Glu]_{dACC}$ × prior beliefs, and 7) $[Glu]_{dACC}$ × precision of PEs as covariates. All but the behavioral model (see below) were reduced versions of the 3-level model.

A no-glutamate model represented the hypothesis that $[Glu]_{dACC}$ did not affect the network's effective connectivity. Neither the main effect of $[Glu]_{dACC}$ nor the $[Glu]_{dACC}$ × group interaction was included in the model. A no-computational model did not include the effects of prior beliefs, precision of PE, prior beliefs × group, and precision of PEs × group. It represented the hypothesis that prior beliefs and precision of PEs do not affect connectivity. A behavioral model substituted (in the 3-level model) the behavioral responses and their interactions with group for the hierarchical drift-diffusion model parameters. This model represented the hypothesis that the observed responses better account for network connectivity than the computational parameters. For completeness, we fit a group model (with only the main effect of group representing the hypothesis that only differences between groups would cause changes in the network connectivity) and a null model (representing the hypothesis of no effect of covariates on the network). To adjudicate between models, we performed a Bayesian model comparison (44). To evaluate our 3-level hypothesis, we report the effect sizes (i.e., parameters of the between-subject parametric empirical Bayesian model associated with each covariate along with the posterior probabilities). A data analysis pipeline is detailed in Figure S2.

RESULTS

Participants performed the task as instructed. As expected, in the incongruent condition, subjects with FEP were less accurate and took longer than HC subjects (Table 1 and Table S4). The hierarchical drift-diffusion model showed that the drift-rate parameter in the HC group (mean = 2.83, SD = 0.18) was larger than in the FEP group (mean = 1.83, SD = 0.2). The difference in PP was = 0.99. The starting point in the FEP group was larger (i.e., closer to the decision boundary, mean = 0.44, SD = 0.03) than in the HC group (mean = 0.32, SD = 0.03; difference in PP = 0.99). The decision threshold was lower in the FEP group (mean = 2.06, SD = 0.32) than in the HC group (mean = 2.52, SD = 0.09; difference in PP = 0.96). Finally, the nondecision processes took longer in the FEP group (mean = 0.64, SD = 0.11) than in the HC group (mean = 0.46, SD = 0.09; difference in PP = 0.99; Figure S3 and Tables S5 and S6).

$[Glu]_{dACC}$ Affects Intrinsic Inhibitory Connections in Core Nodes of the Salience Network

The 3-level model outperformed all the alternative models (Figure 2 and Table S7). The mean estimates across groups revealed inhibition in both regions (dACC, mean = 2.35, PP = 1.0; AI, mean = 2.51, PP = 1.0) and an attenuation in the strength of excitatory connections (dACC → AI, mean = −0.51, PP = 0.99; AI → dACC, mean = −0.45, PP = 0.99). Figure 3 shows no main effect of group on parameters. However, main effect of $[Glu]_{dACC}$ on self-connections in both regions was

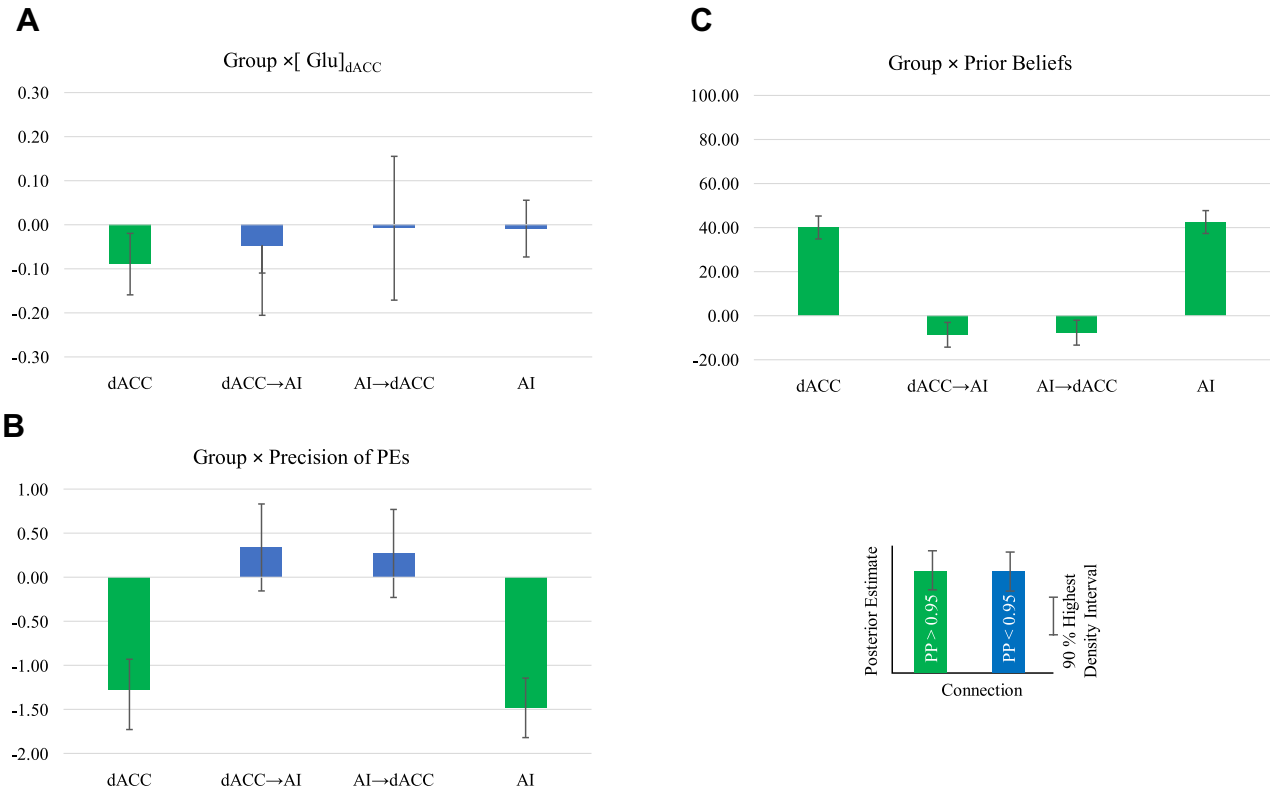

Figure 4. Interactions between group and covariates in the winning 3-level parametric empirical Bayes model. Panel **(A)** shows the effect of group on connections modulated by $[Glu]_{dACC}$. Panels **(B)** and **(C)** show the effect of group modulated by the precision of prediction errors (PEs) and prior beliefs, respectively. Positive values represent stronger effect in the first-episode psychosis group, and vice versa. AI, anterior insula; dACC, dorsal anterior cingulate cortex; $[Glu]_{dACC}$, glutamate in the dorsal anterior cingulate cortex; PP, posterior probability.

detected. Intrinsic inhibition increased in the dACC ($\beta = 0.11$, PP = 0.99) and decreased in the AI ($\beta = -0.07$, PP = 0.96). Prior beliefs did not affect extrinsic connections. However, precision of PEs strengthened inhibitory connections (dACC, $\beta = 0.92$, PP = 1; AI, $\beta = 1.1$, PP = 1).

$[Glu]_{dACC}$ Correlates Negatively With Intrinsic Inhibitory Influence in the dACC of Subjects With FEP, Accounting for Aberrant Prior Beliefs and Aberrant Precision of PE

Figure 4 shows that in the dACC, $[Glu]_{dACC}$ was associated with weaker inhibitory connections in the FEP group than in the HC group ($\beta = -0.09$, PP = 0.98), and that the effect of prior beliefs on inhibitory connections was stronger in the FEP group than in the HC group (dACC, $\beta = 40.01$, PP = 1; AI, $\beta = 42.48$, PP = 1). Surprisingly, the effect of prior beliefs on excitatory connections was weaker in the FEP group than in the HC group (dACC → AI, $\beta = -8.72$, PP = 0.99; AI → dACC, $\beta = -7.76$, PP = 0.99). Finally, we found that the effect of precision of PEs on inhibitory connections was weaker in subjects with FEP than in HC participants (dACC, $\beta = -1.28$, PP = 1; AI, $\beta = -1.48$, PP = 1). In summary, $[Glu]_{dACC}$ differentially affected the network's effective connectivity, which was differentially associated with the parameter estimates of the hierarchical drift-diffusion model in the presence of FEP.

Connectivity Strength Correlates Negatively With Severity of Social Withdrawal

We searched for negative association between the severity of blunted affect, social withdrawal, and lack of spontaneity and the strength of connections in the FEP group. We made 3 comparisons per connection (Bonferroni correction, $p = .017$). Only the effect of backward connections on social withdrawal survived correction. Severity of social withdrawal increased as the connectivity strength of dACC → AI connections decreased (Figure 5). For completeness, we also explored the association between hallucinations and delusions and connectivity strength (2 comparisons per connection with Bonferroni correction, $p = .025$). None of the comparisons reached statistical significance at this level of correction.

DISCUSSION

We have demonstrated that low computational performance during cognitive-conflict resolution in FEP is explained by aberrant resting-state effective connectivity (dysconnection) in core nodes of the salience network (dACC and AI). This dysconnection was associated with glutamate hypofunction in the dACC, as proven by the fact that a model without the effect of $[Glu]_{dACC}$ had low probability of explaining the fMRI data. $[Glu]_{dACC}$ was associated with opposite intrinsic connectivity strength in both the dACC and the AI, indicating that $[Glu]_{dACC}$ affected the entire network and confirming the sensitivity of the

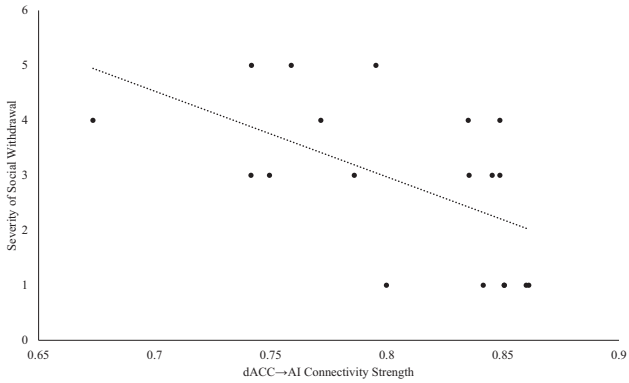

Figure 5. Association between extrinsic connectivity strength and severity of social withdrawal. $\beta = -15.59$, SE = 5.61, $t_{16} = 2.78$, $p = .013$, 95% confidence interval (27.43–3.75). AI, anterior insula; dACC, dorsal anterior cingulate cortex.

AI to changes in the dACC excitation-inhibition balance. Crucially, in the FEP group the inhibitory influence on the excitatory population of the dACC decreased as a function of $[Glu]_{dACC}$. This finding is the first imaging evidence directly linking the glutamate hypofunction to the cortical disinhibition hypothesis in schizophrenia.

Decreased intrinsic inhibition and decreased extrinsic connectivity have been previously reported in the default mode (46) and dorsal attention networks (47) of subjects with schizophrenia. The fact that 3 independent groups have shown the same relationship between decreased intrinsic and extrinsic connections in the default mode, attention, and salience networks provides strong support to the dysconnection hypothesis of schizophrenia. Crucially, our results point to glutamate hypofunction and aberrant computations of sensory and prior precision as critical causes of dysconnection and are in line with recently reported data showing that the effect of glutamate hypofunction should be observed at the network level (48).

These results also demonstrate that establishing the relationship between glutamate hypofunction, the disinhibition hypothesis, and the pathophysiology of schizophrenia requires the integration of the neurochemical, effective-connectivity, and computational levels of analysis—since Bayesian model comparison afforded low probability to any model not comprising all 3 levels. Specifically, parameter estimates of resting-state aberrant connectivity (driven by resting-state $[Glu]_{dACC}$) in the dACC–AI network account for computational parameters of cognitive dysfunction in FEP. Furthermore, an increase in the effect of the inhibitory population on the excitatory population in both regions explains the precision subjects afforded to ascending information, in line with the known role of GABA interneurons in pyramidal circuits (49).

The 3-level hypothesis also explains the computational compensatory effect of aberrant prior beliefs to aberrant precision of ascending information in subjects with FEP. They needed to accumulate less information than HC subjects (i.e., lower decision threshold), relied more on their prior beliefs (i.e., at the beginning of each trial they were closer to the decision boundary) than on sensory information, and were less cautious when resolving cognitive conflicts—they tended to jump to conclusions (50). At a group level, we did not find evidence for a larger precision of PEs in the FEP group than in the HC group. On the contrary, the HC group showed a steeper drift rate. However, within the FEP group aberrant precision PEs was associated with a decrease in the strength of inhibitory connections in both regions (Figure 4B). Crucially, an increase in the inhibitory activity was associated with an increase in prior beliefs (Figure 4C), suggesting (at the effective-connectivity level) that more precise prior beliefs compensate for aberrant precision of PEs as predicted by the dysconnection hypothesis (7).

The current results are in concert with a previous study that used 4-neuronal-population DCM to model GABA connections to superficial pyramidal cells (9). In the referred work, model parameters were associated with behavioral performance, showing that establishing a relationship between synaptic dysfunction and behavior requires modeling effective connectivity. However, our 3-level model outperformed a model including behavioral observations, suggesting that symptoms of schizophrenia emerge from the interaction between neurochemical, network-connectivity, and computational variables.

Another previous work has reported no relationship between $[Glu]_{dACC}$ and deficits in Stroop performance in subjects with FEP (20). However, unlike our study, it included neither the network nor the computational level of analysis. These 2 levels allowed us to observe the indirect effect of $[Glu]_{dACC}$ on Stroop computations through the aberrant effective connectivity within the dACC–AI network. Similarly, a recent Bayesian study has suggested that prior beliefs might not influence behavioral performance in the absence of sensory stimulation (51). Our subjects with FEP did not expect sensory stimulation. However, the weaker the connectivity strength in descending connections (representing prior beliefs) was in resting state, the more biased were subjects' responses toward the decision threshold in the Stroop task. Therefore, it is possible that the effect that prior beliefs might exert on behavioral performance depends not only on the sensory stimulation but also on the resting-state connectivity strength of descending connections.

As per the dysconnection hypothesis, the negative correlation between the dACC → AI connectivity strength and severity of social withdrawal appears counterintuitive: on the one hand, overly afforded confidence in prior beliefs would be expected to correlate positively with increased strength in descending connections, whereas on the other hand, increased connectivity strength should correlate positively with negative symptom severity. It is important to note that we observed a relationship between strong prior beliefs and reduced dACC → AI connectivity that relates to social withdrawal. In fact, stronger priors relate to both reduced dACC → AI connectivity and increased intrinsic inhibitory tone of dACC and AI. This relationship is consistent with an effective connectivity study that relates intrinsic inhibitory connections within primary visual cortex and negative symptoms. Moreover, recent models of effortful control (52) suggest that strong priors along with top-down dysconnectivity may relate to a reduced effort signal from the dACC to the AI and thus present as motivational deficits indexed by social withdrawal. While our data do not support the predictions of a direct relationship between strong prior

beliefs and negative symptoms severity, it is worth noting that our resting-state experimental setup did not allow for the suboptimal Bayesian agent (the patient) to withdraw from a social environment that is rich in sensory stimulation. From the perspective of active inference under the free-energy formulation, there is no social withdrawal in a dark room (53).

Within the context of these previous works, a negative correlation between connectivity strength and negative symptoms appears to be explained not only by the general active inference theory under the free-energy formulation but also in terms of utility models [as special cases of active inference (54)]. However, because the works showing an association between high prior beliefs, weak connections, and negative symptoms are scarce and equivocal [e.g., a recent functional connectivity work found no association between connections in the salience network and negative symptoms (55)], this association should be taken as a working hypothesis.

Limitations and Future Directions

Our 3-level hypothesis was tested via hierarchical Bayesian inference, which considers the data hierarchy and uses informative prior distributions and shrinkage. Therefore, within the assumptions of Bayesian statistics, the posterior probabilities of our estimates showed large and reliable effect sizes. Nevertheless, the current sample size could be regarded as small for classical inferences such as those pertaining to the between-group differential effect of $[Glu]_{dACC}$ and the association between symptoms and connectivity strength.

With resting-state fMRI, we controlled for task as a confounding factor of the effect of $[Glu]_{dACC}$ on inhibitory connections. Since the current results show this effect, future studies could address the task $\times$ glutamate interaction. By combining task fMRI with 4 neuronal-population DCM, it would be possible to set the effect of $[Glu]_{dACC}$ on inhibitory connections as priors while modeling the effect of glutamate in other regions. One region that could be added to the current network is the ventrolateral prefrontal cortex, which, along with the AI and the dACC, is engaged by interference and cognitive control processes during the Stroop task. In the context of hierarchical message passing, 4 neuronal-population DCM would allow to investigate the hierarchical relationship between the dACC and ventrolateral prefrontal cortex,[2] by testing different hierarchical connections between superficial and deep pyramidal cells across regions.

Conclusions

This work provides evidence to the hypothesis that the glutamate hypofunction relies on the disinhibition hypothesis and manifests itself in the effective connectivity of key nodes of the salience network. The 3-level hypothesis provides compelling explanation to deficits in cognitive control and negative symptoms in schizophrenia. The findings support a link between glutamate-mediated cortical disinhibition, deficits in effective connectivity, and computational performance in FEP.

[2]We thank an anonymous reviewer for suggesting this future study.

ACKNOWLEDGMENTS AND DISCLOSURES

This study was funded by CIHR Foundation Grant No. 375104/2017 (to LP); Schulich School of Medicine Clinical Investigator Fellowship (to KD); AMOSO Opportunities fund to LP; Bucke Family Fund (to LP); BrainSCAN (to RL); grad student salary support of PJ by NSERC Discovery Grant No. RGPIN2016-05055 (to JT); Canada Graduate Scholarship (to KD). Data acquisition was supported by the Canada First Excellence Research Fund to BrainSCAN, Western University (Imaging Core); Innovation fund for Academic Medical Organization of Southwest Ontario; Bucke Family Fund, The Chrysalis Foundation and The Arcangelo Rea Family Foundation (London, Ontario).

We thank Dr. Joe Gati, Mr. Trevor Szekeres, and Dr. Ali Khan for their assistance in data acquisition and archiving. We thank Dr. Maria Densmore for producing supplementary SPM (statistical parametric mapping) outputs. We thank Dr. William Pavlovsky for consultations on clinical radiological queries. We thank an anonymous reviewer for providing compelling recommendations on the first draft of this work. We thank Drs. Raj Harricharan, Julie Richard, Priya Subramanian, and Hooman Ganjavi and all staff members of the PEPP London team for their assistance in patient recruitment and supporting clinical care. We gratefully acknowledge the participants and their family members for their contributions.

This article was published as preprint on bioRxiv: doi:10.1101/828558v1.

LP reports personal fees from Otsuka Canada, SPMM Course Limited, UK, Canadian Psychiatric Association; book royalties from Oxford University Press; investigator-initiated educational grants from Janssen Canada, Sunovion and Otsuka Canada outside the submitted work. All other authors report no biomedical financial interests or potential conflicts of interest.

ARTICLE INFORMATION

From the Department of Psychiatry (RL, MM, JT, LP), Robarts Research Institute (RL, MM, LP), Department of Medical Biophysics (PJ, JT, RB), Department of Medical Imaging (JT), and Schulich School of Medicine and Dentistry (DW), Western University, London; Lawson Health Research Institute (LP), London; Department of Strategic Enterprise Solutions (TD), Fanshawe College, London; Neuropsychiatry Imaging Lab (JT), Lawson Health Research Institute, London; Department of Diagnostic Imaging (JT), St. Joseph's Health Care London, London; and Department of Psychiatry (KD), Dalhousie University, Halifax, Nova Scotia, Canada.

Address correspondence to Roberto Limongi, Ph.D., or Lena Palaniyappan, Ph.D., Robarts Research Institute, 1151 Richmond St. N, UWO, London, Ontario, Canada, N6A 5B7; E-mail: rlimongi@uwo.ca (RL) or lpalaniy@uwo.ca (LP).

Received Sep 16, 2019; revised Jan 6, 2020; accepted Jan 27, 2020.

Supplementary material cited in this article is available online at https://doi.org/10.1016/j.biopsych.2020.01.021.

REFERENCES

1. Coyle JT (1996): The glutamatergic dysfunction hypothesis for schizophrenia. Harv Rev Psychiatry 3:241–253.
2. Olney JW, Farber NB (1995): Glutamate receptor dysfunction and schizophrenia. Arch Gen Psychiatry 52:998–1007.
3. Snyder MA, Gao W-J (2013): NMDA hypofunction as a convergence point for progression and symptoms of schizophrenia. Front Cell Neurosci 7:31.
4. Snyder MA, Gao W-J (2020): NMDA receptor hypofunction for schizophrenia revisited: Perspectives from epigenetic mechanisms. Schizophr Res 217:60–70.
5. Homayoun H, Moghaddam B (2007): NMDA receptor hypofunction produces opposite effects on prefrontal cortex interneurons and pyramidal neurons. J Neurosci 27:11496.
6. Gonzalez-Burgos G, Lewis DA (2008): GABA neurons and the mechanisms of network oscillations: Implications for understanding cortical dysfunction in schizophrenia. Schizophr Bull 34:944–961.
7. Friston KJ, Brown HR, Siemerkus J, Stephan KE (2016): The dysconnection hypothesis (2016). Schizophr Res 176:83–94.
8. Friston KJ (2012): The history of the future of the Bayesian brain. Neuroimage 62:1230–1233.

9. Shaw AD, Knight L, Freeman TCA, Williams GM, Moran RJ, Friston KJ, *et al.* (2020): Oscillatory, computational, and behavioral evidence for impaired GABAergic inhibition in schizophrenia. Schizophr Bull 46:345–353.
10. Spratling MW (2017): A review of predictive coding algorithms. Brain Cogn 112:92–97.
11. Bastos AM, Usrey WM, Adams RA, Mangun GR, Fries P, Friston KJ (2012): Canonical microcircuits for predictive coding. Neuron 76:695–711.
12. Aitchison L, Lengyel M (2017): With or without you: Predictive coding and Bayesian inference in the brain. Curr Opin Neurobiol 46:219–227.
13. Limongi R, Bohaterewicz B, Nowicka M, Plewka A, Friston KJ (2018): Knowing when to stop: Aberrant precision and evidence accumulation in schizophrenia. Schizophr Res 197:386–391.
14. Powers AR 3rd, Gancsos MG, Finn ES, Morgan PT, Corlett PR (2015): Ketamine-induced hallucinations. Psychopathology 48:376–385.
15. Powers AR, Mathys C, Corlett PR (2017): Pavlovian conditioning–induced hallucinations result from overweighting of perceptual priors. Science 357:596–600.
16. Stroop JR (1935): Studies of interference in serial verbal reactions. J Exp Psychol 18:643–662.
17. Wang X, Wang T, Chen Z, Hitchman G, Liu Y, Chen A (2015): Functional connectivity patterns reflect individual differences in conflict adaptation. Neuropsychologia 70:177–184.
18. Shapira-Lichter I, Strauss I, Oren N, Gazit T, Sammartino F, Giacobbe P, *et al.* (2018): Conflict monitoring mechanism at the single-neuron level in the human ventral anterior cingulate cortex. Neuroimage 175:45–55.
19. Taylor R, Théberge J, Williamson PC, Densmore M, Neufeld RWJ (2016): ACC neuro-over-connectivity is associated with mathematically modeled additional encoding operations of schizophrenia Stroop-task performance. Front Psychol 7:1295–1295.
20. Taylor R, Neufeld RWJ, Schaefer B, Densmore M, Rajakumar N, Osuch EA, *et al.* (2015): Functional magnetic resonance spectroscopy of glutamate in schizophrenia and major depressive disorder: Anterior cingulate activity during a color-word Stroop task. NPJ Schizophr 1:15028.
21. Bitzer S, Park H, Blankenburg F, Kiebel S (2014): Perceptual decision making: drift-diffusion model is equivalent to a Bayesian model. Front Hum Neurosci 8:102.
22. Sporns O, Kötter R (2004): Motifs in brain networks. PLoS Biol 2:e369.
23. Pardo JV, Pardo PJ, Janer KW, Raichle ME (1990): The anterior cingulate cortex mediates processing selection in the Stroop attentional conflict paradigm. Proc Natl Acad Sci U S A 87:256–259.
24. Evrard HC, Forro T, Logothetis NK (2012): Von economo neurons in the anterior insula of the macaque monkey. Neuron 74:482–489.
25. Mesulam MM, Mufson EJ (1982): Insula of the old world monkey. III: Efferent cortical output and comments on function. J Comp Neurol 212:38–52.
26. Mufson EJ, Mesulam MM (1982): Insula of the old world monkey. II: Afferent cortical input and comments on the claustrum. J Comp Neurol 212:23–37.
27. Palaniyappan L, Liddle PF (2012): Does the salience network play a cardinal role in psychosis? An emerging hypothesis of insular dysfunction. J Psychiatry Neurosci 2012;37:17–27.
28. Palaniyappan L, Simmonite M, White TP, Liddle EB, Liddle PF (2013): Neural primacy of the salience processing system in schizophrenia. Neuron 79:814–828.
29. Moran LV, Tagamets MA, Sampath H, O'Donnell A, Stein EA, Kochunov P, *et al.* (2013): Disruption of anterior insula modulation of large-scale brain networks in schizophrenia. Biol Psychiatry 74:467–474.
30. Limongi R, Sutherland SC, Zhu J, Young ME, Habib R (2013): Temporal prediction errors modulate cingulate-insular coupling. Neuroimage 71:147–157.
31. Merritt K, McGuire P, Egerton A (2013): Relationship between glutamate dysfunction and symptoms and cognitive function in psychosis. Front Psychiatry 4:151–151.
32. Adams R, Stephan K, Brown H, Frith C, Friston K (2013): The computational anatomy of psychosis. Front Psychiatry 4:47.
33. Valton V, Romaniuk L, Douglas Steele J, Lawrie S, Seriès P (2017): Comprehensive review: Computational modelling of schizophrenia. Neurosci Biobehav Rev 83:631–646.
34. Jardri R, Denève S (2013): Circular inferences in schizophrenia. Brain 136:3227–3241.
35. Psychiatric Association (2013): Diagnostic and Statistical Manual of Mental Disorders, 5th ed. American Psychiatric Press, Washington, DC.
36. Leckman JF, Sholomskas D, Thompson WD, Belanger A, Weissman MM (1982): Best estimate of lifetime psychiatric diagnosis: A methodological study. Arch Gen Psychiatry 39:879–883.
37. Andreasen NC, Carpenter WTJ, Kane JM, Lasser RA, Marder SR, Weinberger DR (2005): Remission in schizophrenia: proposed criteria and rationale for consensus. Am J Psychiatry 162:441–449.
38. Wong D, Schranz AL, Bartha R (2018): Optimized in vivo brain glutamate measurement using long-echo-time semi-LASER at 7 T. NMR Biomed 31:e4002.
39. Fard PR, Park H, Warkentin A, Kiebel SJ, Bitzer S (2017): A Bayesian reformulation of the extended drift-diffusion model in perceptual decision making. Front Comput Neurosci 11:29.
40. Marreiros AC, Kiebel SJ, Friston KJ (2008): Dynamic causal modelling for fMRI: A two-state model. Neuroimage 39:269–278.
41. Razi A, Kahan J, Rees G, Friston KJ (2015): Construct validation of a DCM for resting state fMRI. Neuroimage 106:1–14.
42. Kahan J, Urner M, Moran R, Flandin G, Marreiros A, Mancini L, *et al.* (2014): Resting state functional MRI in Parkinson's disease: the impact of deep brain stimulation on "effective" connectivity. Brain 137:1130–1144.
43. Limongi R, Perez FJ, Modrono C, Gonzalez-Mora JL (2016): Temporal uncertainty and temporal estimation errors affect insular activity and the frontostriatal indirect pathway during action update: a predictive coding study. Front Human Neurosci 10:276.
44. Friston KJ, Litvak V, Oswal A, Razi A, Stephan KE, van Wijk BCM, *et al.* (2016): Bayesian model reduction and empirical Bayes for group (DCM) studies. Neuroimage 128:413–431.
45. Zeidman P, Jafarian A, Seghier ML, Litvak V, Cagnan H, Price CJ, *et al.* (2019): A guide to group effective connectivity analysis, part 2: Second level analysis with PEB. Neuroimage 200:12–25.
46. Bastos-Leite AJ, Ridgway GR, Silveira C, Norton A, Reis S, Friston KJ (2015): Dysconnectivity within the default mode in first-episode schizophrenia: A stochastic dynamic causal modeling study with functional magnetic resonance imaging. Schizophr Bull 41:144–153.
47. Zhou Y, Zeidman P, Wu S, Razi A, Chen C, Yang L, *et al.* (2018): Altered intrinsic and extrinsic connectivity in schizophrenia. Neuroimage Clin 17:704–716.
48. Bryant JE, Frölich M, Tran S, Reid MA, Lahti AC, Kraguljac NV (2019): Ketamine induced changes in regional cerebral blood flow, interregional connectivity patterns, and glutamate metabolism. J Psychiatr Res 117:108–115.
49. Tremblay R, Lee S, Rudy B (2016): GABAergic interneurons in the neocortex: From cellular properties to circuits. Neuron 91:260–292.
50. Evans SL, Averbeck BB, Furl N (2015): Jumping to conclusions in schizophrenia. Neuropsychiatr Dis Treat 11:1615–1624.
51. Valton V, Karvelis P, Richards KL, Seitz AR, Lawrie SM, Seriès P (2019): Acquisition of visual priors and induced hallucinations in chronic schizophrenia. Brain 142:2523–2537.
52. André N, Audiffren M, Baumeister RF (2019): An integrative model of effortful control. Front Syst Neurosci 13:79.
53. Friston K, Thornton C, Clark A (2012): Free-energy minimization and the dark-room problem. Frontiers in psychology 3:130–130.
54. Friston KJ, Daunizeau J, Kiebel SJ (2009): Reinforcement learning or active inference? PLoS One 4:e6421.
55. Supekar K, Cai W, Krishnadas R, Palaniyappan L, Menon V (2019): Dysregulated brain dynamics in a triple-network saliency model of schizophrenia and its relation to psychosis. Biol Psychiatry 85:60–69.